Low resistance transparent electrodes for large area flat display devices

S. J. Laverty[a] and P. D. Maguire
School of Electrical and Mechanical Engineering, University of Ulster, Newtownabbey, County Antrim BT37 0QB, Northern Ireland

(Received 26 May 2000; accepted 30 October 2000)

The dynamic performance of large area, high-resolution flat panel displays is contingent upon the conductivity of the transparent electrode. Electroplated copper and vacuum deposited aluminum bus bars attached to the sidewalls of conventional SnO_2 electrodes offer theoretical improvements in conductivity while maintaining the electrode transmittivity. In association with a reactive ion etching process for delineating the tin oxide, auto registration methods for attaching copper by electroplating and aluminum by a resist lift off process are described, together with the achieved enhancement factors. A contact resistance between the aluminum and the tin oxide was found to significantly reduce the enhancement. The sidewall contact resistance lies between 0.4 and 4.0 $\times 10^4\ \Omega\ \mu m^2$, considerably lower than that previously reported for contacts to the tin oxide top surface. The enhancement factor for aluminum lies between two and three. The application of copper did not suffer from a contact resistance and an order of magnitude enhancement was obtained. We also report excellent adhesion, typically greater than 200 kg/cm^2, of the metals to the tin oxide and identify the parametric space for achieving this. © *2001 American Vacuum Society.*
[DOI: 10.1116/1.1335676]

I. INTRODUCTION

Large area and high-resolution, liquid crystal, electroluminescent and plasma displays demand a dynamic performance conditioned in part by the transmission line properties of the electrodes linking the drive electronics to the pixel. Electrically, the orthogonal electrodes of the display are nonlinear capacitively loaded transmission lines[1] and pixel response time, brightness uniformity, and energy transfer all depend critically on transmission bandwidth and the conditioning electrode line resistance.[2] In LCD panels this resistance can be as high as 120 kΩ[3] and here dynamic performance is sustained by a TFT active matrix design. Line resistance also factors into power consumption and is thus of significance to the design and efficiency of photovoltaic solar panels. In these optoelectronic applications, transparency of the front electrode is essential to efficient operation with the result that tin oxide (TO, SnO_2) and indium tin oxide (ITO, In_2O_3:Sn), which offer the best compromise between transparency and conductivity, are the widely used front electrode materials. Conductivity, transparency, their interdependence,[4,5] and the ability to delineate the transparent electrode, are not readily compatible. Doping the metal oxide, e.g., SnO_2:F, is the standard route to improved conductivity by enhancing carrier density. In a recent work,[6] this approach has achieved nearly an order of magnitude improvement in conductivity with transmittivity held at 85% but impurity scattering is expected to limit the minimum resistivity to the low $10^{-4}\ \Omega^1\ cm^1$ region. Compared to low resistance metals such as copper and aluminum, with resistivity approaching $10^{-6}\ \Omega$ cm, the intrinsic oxide resistivity is expected to remain at up to two orders of magnitude higher. Typical 90% transparent SnO_2 films have a minimum sheet resistance of 10 $\Omega/\square$, corresponding to a resistivity of about 200–400 $\mu\Omega$ cm, which is too high for large area panels without some form of conductivity enhancement. Hence a sheet resistance around 1 $\Omega/\square$, without a significant decrease in transmittivity, is to be aimed for.

With limited prospects for reduced intrinsic resistivity alternative strategies must be pursued. One such alternative, proposed by Hope,[7] involves a hybrid electrode structure using a thin aluminum stripe in contact with the surface of the indium tin oxide electrode. While conceptually straightforward, this approach does partially obscure the underlying transparent electrode and also results in a nonplanar topology. An adaptation that is the subject of our studies is to attach the low resistance bus bar to the vertical sidewalls of the electrode in the interelectrode gap. The required resolution of a display is determined by the response of the eye and since the perceived visual quality of a display image does not improve at resolutions beyond 4 lines/mm, the ultimate minimum electrode pitch and gap are set at about 100 and 10 μm, respectively. These feature sizes are large compared to the capability of standard photolithography and provide ample scope for metallization within the interelectrode gap without significant added complexity or cost.

Two methods are presented: copper attachment by electrochemical processing, as shown in Fig. 1(a), and aluminum attachment by a resist lift-off process, Fig. 1(b). Both processes are self-aligning with the latter requiring an additional noncritical photomasking and etch step to create isolation channels between adjacent electrodes. Electroplating is a potential low cost nonvacuum process for very large area plasma panels whereas vacuum metal deposition may be more appropriate for very high-resolution displays.

[a]Electronic mail: sj.laverty@ulst.ac.uk

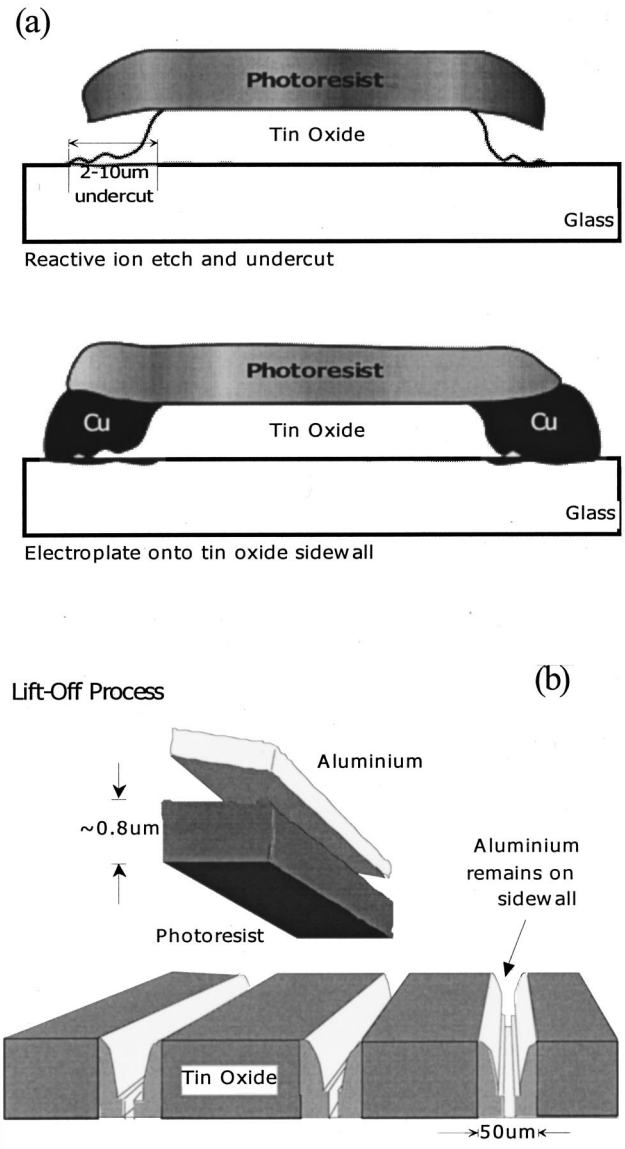

FIG. 1. Sidewall attachment of metals to a RIE delineated tin oxide electrode. (a) Copper attachment by electrolytic etching which undercuts the resist, followed by electroplating of copper. The resist overhang constrains vertical copper growth to leave a final electrode that is almost planar. (b) Aluminum attachment by a resist lift-off and aluminum fracture process. An additional delineation of the aluminum is needed to separate adjacent electrodes.

II. EXPERIMENT

Soda glass substrates coated with fluorine doped chemical vapor deposited tin oxide were used as the vehicle for evaluating the concept. The resistivity and thickness of the tin oxide were 8–16 Ω/ and 320–400 nm, respectively. Delineation of the electrode patterns was achieved using Dynachem OFPR800FP photoresist and an argon-chlorine reactive ion etch[8] with typical process parameters being: 9:1 $Ar–Cl_2$ gas mixture at a working pressure of 80 mTorr, and an input power of 350 W, developing a dc bias of 450 V. The electrodes were patterned at 50 lines/in with a linewidth to pitch ratio (fill factor) of 90%. At these dimensions, typical tin oxide etch rates were at least 70 nm/min. The differential etch rate of resist and tin oxide is approximately 2:1, with the resist etching much faster than the tin oxide. Loading effects require this value to be adjusted upwards for lower fill factors.[9] The resist was deposited using a large area flood and drain system that allows uniform thickness control from 0.5 to 2 μm. The initial thickness was adjusted to account for resist loss during the etch process and the optimum postetch thicknesses were found to be 450 and 800 nm for the copper and aluminum processes, respectively. An increase in the adhesion of the aluminum, typically about 50 kg/cm^2, to the roughened surface of the plasma bombarded resist was found to enhance the lift-off compared to a number of nonplasma chemical etch processes investigated. Adhesion was measured in the *z*-axis pull mode using a Sebastian Five-A rate and load application unit.

A. Aluminum attachment

With 800 nm of resist remaining post-reactive ion etching (RIE), thermally evaporated aluminum films up to 500 nm could be successfully sheered in the lift-off process. In these experiments optimal thickness of the deposited aluminum was in the range 200–400 nm. Talystep and four point probe measurements were used to record thickness and sheet resistivity of the deposited aluminum films, which ranged from 0.57 Ω/□, at 0.1 μm to 0.11 Ω/□ at 0.44 μm. Adhesion to a RIE treated tin oxide surface was generally good, being consistently greater than 200 kg/cm^2. No parametric dependency for aluminum adhesion was observed in these studies.

B. Copper attachment

Copper attachment was carried out in a two-stage process. After RIE delineation of the electrodes, electrolysis in a 0.1 M H_2SO_4 aqueous solution with a current density of 25 mA/cm^2 for 5–10 s duration etches back the tin oxide sidewall resulting in a resist overhang of 2–10 μm. As the etch proceeds, small islands of tin oxide become electrically isolated from the main electrode and thus sustain no further etching. This stage is followed by electroplating in an aqueous solution of copper sulphate (188 g/l) and sulfuric acid (0.6 M) with a copper electrode forming the anode. The previously noted tin oxide islands now become electrically connected by the advancing copper and help anchor the copper to the glass surface. Adhesion, lying between zero and 1000 kg/cm^2, was highly dependent on reduction and plating parameters.

III. RESULTS AND DISCUSSION

A. Aluminum process

In addition to the 50 lines/in. electrodes, groups of three resistivity test patterns, Fig. 2, were distributed over the panel to facilitate measurement of the electrical resistivity of the aluminum, the tin oxide stripe, and a combined tin oxide–aluminum electrode structure. The initial tin oxide resistance, in the structure of Fig. 2(a), was 41–50 Ω reducing to 15–25 Ω, respectively, after attachment of aluminum to the sidewall. The measured enhancement in conductivity was

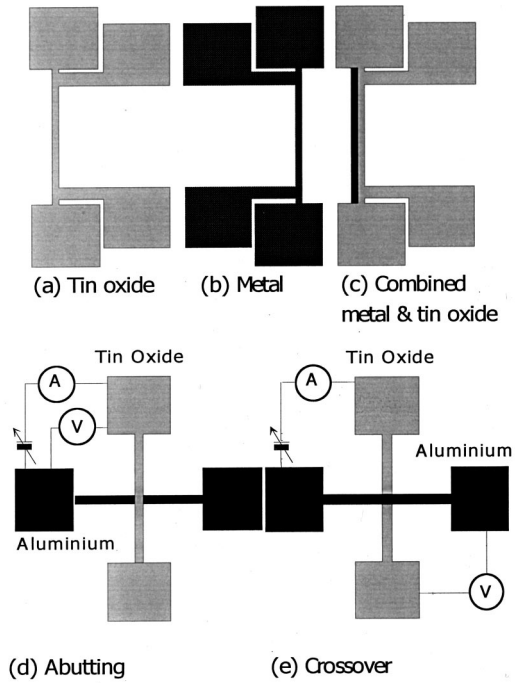

FIG. 2. Test patterns for measuring electrical conductivity of (a) tin oxide, (b) metal, (c) tin oxide with sidewall metal attached, (d) aluminum abutting the sidewall of the tin oxide, and (e) aluminum crossing over the tin oxide top surface.

significantly less than a simple calculation based on parallel resistors, which indicated an expected conductivity enhancement factor lying between 5 and 10. The displacement of the experimental data from that calculated indicates the presence of a relatively constant contact resistance along the sidewall interface between aluminum and tin oxide. Using a lumped resistance model of $\frac{1}{2}R$ at either end of the tin oxide electrode, an estimate of the contact resistance can be obtained by a least-squares fit to the experimental data, Fig. 3. This fit is constrained to have a gradient less than the zero contact resistance calculated slope of 0.84 and the resulting estimate for R is approximately 15 Ω. The associated contact resistivity, allowing for the distributed contact and current crowding near the ends, was calculated to be $0.4–1.0\times10^4$ Ω μm^2.

To further investigate the contact resistance, additional cruciform test devices, Figs. 2(d) and 2(e), consisting of a 200-μm-wide aluminum strip orthogonal to a 200-μm-wide tin oxide electrode in both overlapping and abutting configurations were defined on the panels. Measurement of resistance across the two back to back sidewall contacts (abutting configuration) indicates an average value, over 26 samples, of 1245 Ω (standard deviation 92 Ω). The associated mean value of contact resistivity, making due allowance for the aluminum track in series with the contact, is 3.44×10^4 Ω μm^2. This result is of a similar order of magnitude to contact resistance values determined from the structures of Figs. 1(a)–1(c) and in general the contact resistance was found to be consistent across nine different panels and associated sets of test structures (Fig. 3).

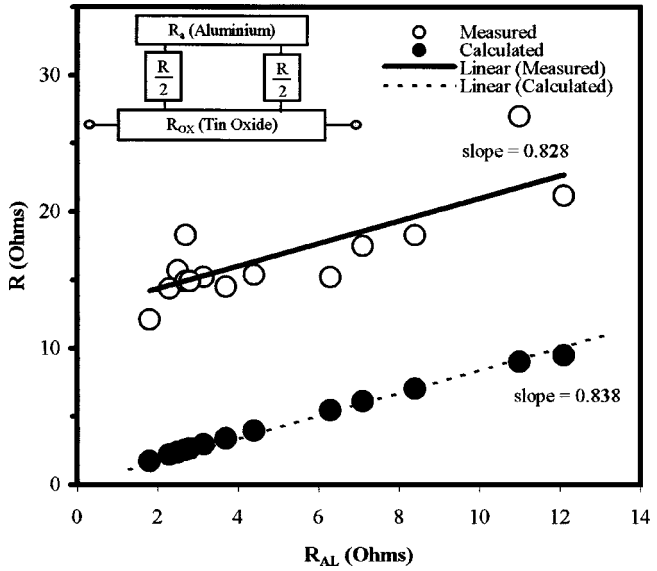

FIG. 3. Experimental and calculated resistance of the combined tin oxide-aluminum electrode. A lumped contact resistance (R/2 in the inset model) of 7.5 Ω yields the solid line drawn through the experimental data.

B. Copper process

The preplating electrolysis stage has been found to enhance adhesion of the copper to the tin oxide while the resulting resist overhang has been found to constrain the copper growth in the direction normal to the panel. Without the overhang the vertical growth rate is equal or greater than the horizontal thus limiting the copper width to ~400 nm, the thickness of the tin oxide. The parameter space for the electrolysis process, encompassing area, current, and time may be represented by a single variable, the per unit area electrical charge Q_R. Typically, as shown in Fig. 4, the removal of the tin oxide increases with Q_R up to about 0.5 mA/cm^2 whereupon saturation sets in. The saturated value increases

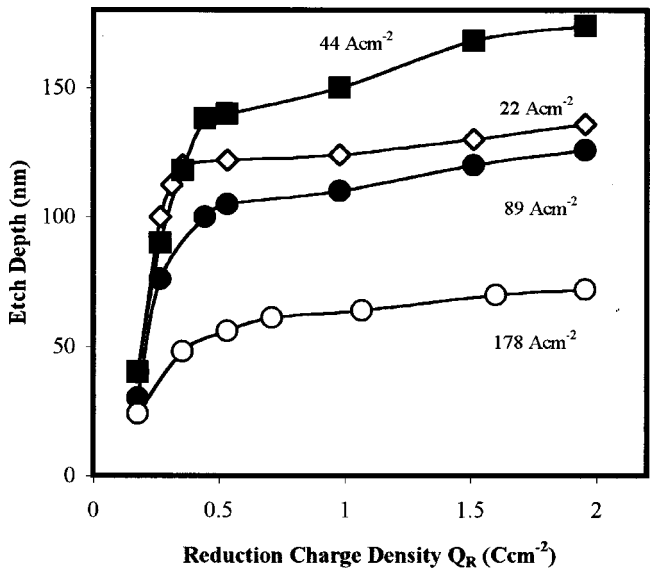

FIG. 4. Etch depth as a function of both the charge density and the current density during electrolysis in the copper process.

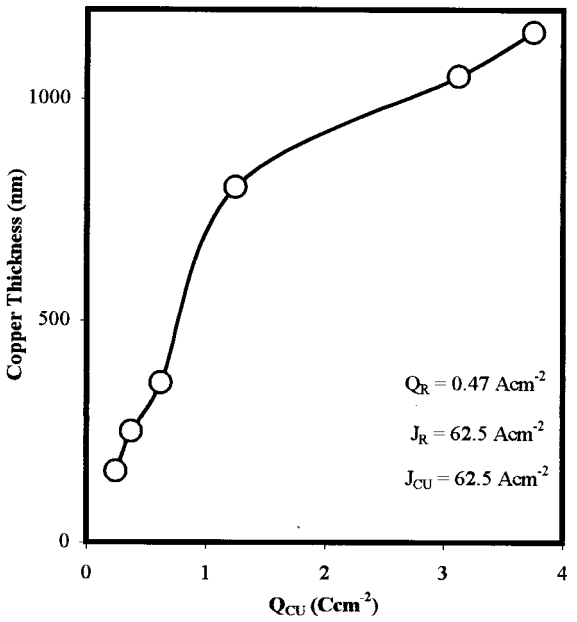

FIG. 5. Copper thickness as a function of the charge density during copper plating process.

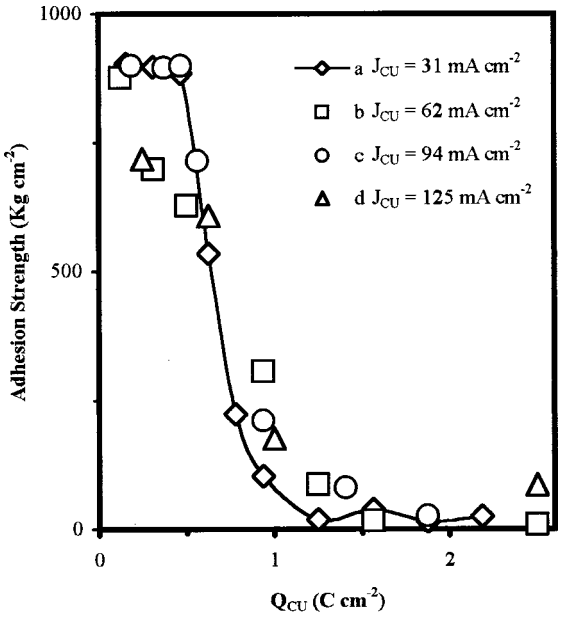

FIG. 6. Variation of the adhesion strength of copper attached to tin oxide over a range of charge and current densities in the copper plating process.

with current density J_R up to 44 mA/cm^2, thereafter decreasing. This decrease at high current densities is due in part to the pattern related potential drop in the panel electrode system and in the 5 μm long by 320 nm high electrochemical channel below the undercut resist. However other surface phenomena must be involved as the copper deposition rate is decreased when Q_R is high. For a given set of electrolysis reduction conditions the copper deposition rate is virtually linear with plating charge density, Fig. 5, although a gradual reduction in gradient at high plating charge density is observed. However, as the reduction charge density Q_R increases from 0.2 to 0.8 C/cm^2 the quantity of copper deposited is found to decrease from 400 to 150 nm. In addition, for a sufficient adhesion strength greater than 200 kg/cm^2, a minimum Q_R of 0.3 C/cm^2 was required. Thus the parameter space, $0.3<Q_R<0.5$ C/cm^2, can be identified as that required to meet both thickness and adhesion constraints. A hyperbolic relationship, Fig. 6, exists between adhesion of the copper and the plating charge density Q_{Cu}. For a minimal adhesion of 200 kg/cm^2, the maximum Q_{Cu} is 1.0 C/cm^2 while the lower limit on Q_{Cu} is 0.3 C/cm^2. Below this limit, the conductivity and appearance of the copper is poor; it exhibits no metallic luster, possibly due to oxidation or incomplete surface coverage.

C. Copper–tin oxide interface

Attachment of the copper to the surface can be due to physisorption, where no significant chemical reaction has occurred, or to chemisorption, whereby a stronger bond is formed. Investigation of the reduced surface, by x-ray photoelectron spectroscopy (XPS),[10] indicates that the initial SnO_2 surface is modified to one which includes Sn^0, Sn^{2+}, and Sn^{4+} species and this surface region increases in thickness as further oxygen is lost. Once the limit of its stability is reached, metal is lost to the electrolyte and/or the transport of reduction species through this layer becomes sufficiently impeded. The latter corresponds to the saturation region in Fig. 4. Below this immediate surface layer, the tin oxidation state is predominately Sn^{4+} with the presence of additional higher binding energy species, possibly due to the formation of hydroxylated tin oxide, $Sn(OH)_4$. X-ray diffraction (XRD)[10] indicates predominantly polycrystalline (200) tin oxide but after reduction the dominance of (200) is greatly reduced, (110) is increased, and extra peaks consistent with β-Sn are observed. It has been suggested[11] that reduction causes preferential (200) etching. However atomic force microscopy (AFM) displayed a roughness of 40 nm (rms), which is not a sufficient topology change to support this and furthermore, heating in oxygen returns the (200) peak to its original value. A more probable explanation is progressive removal of the relatively inert (200) plane's surface and interstitial oxygen giving rise to surface features dominated by exposed (110) planes, possibly to the depth of the measured roughness, 40 nm. X-ray absorption due to the consequential surface scattering could thus account for the apparent anomaly of XRD with a 500 nm range exhibiting such sensitivity to surface modifications. Charge neutrality on the (110) plane requires partial conversion of the Sn^{4+} to Sn^{2+} oxidation state. Achieving this increased reactivity may be the causal factor essential to a strong copper–tin bond.

XRD analysis of the surface gave the texture coefficients for the tin oxide before reduction as 0.21 for (110) and 2.63 for (200) and after reduction as 0.42 for (110) and 1.35 for (200). Besides being rougher than the (200) (rms 10 nm) plane, the resistance of a tin oxide surface with (110) (rms 60 nm) orientation is higher than that for (200) because of the likely presence of Sn^{2+}, which gives rise to traps. In addi-

tion to AFM, four point probe resistivity measurements also correlate with the increased texture coefficient for the (110) plane. The electrolytic formation of a rougher and less inert surface is consistent with the dependence of copper adhesion on Q_R. Copper plating proved to be more successful in enhancing the electrode conductivity than the competing aluminum lift-off process. No contact resistance was observed in the copper case as compared to a significant Al contact resistance of $1.0-4.0\times10^4\ \Omega\ \mu m^2$. Consequently the copper process reduced the effective electrode sheet resistivity from 10 to 0.5 $\Omega/\square$, a conductivity enhancement factor of 20 while the best achieved with the aluminum was a factor of 2.5, with the reduction in sheet resistance to 4.0 $\Omega/\square$.

D. Aluminum–tin oxide interface

Adhesion in the aluminum process was consistently above 500 kg/cm^2, similar to that observed for the optimized sidewall copper. This excellent adhesion has been attributed to the surface conditioning[12] brought about by the RIE in a manner similar to the electrolysis reduction stage in the copper process, which leaves a tin enriched surface[5,13] which further enhances the kinetics of copper plating. The RIE plasma consists of the complementary mechanisms of Ar ion bombardment and chemical attachment of Cl to form the volatile $SnCl_2/SnCl_4$ species. The argon bombardment conditions the normally inert surface to enhance chlorine reactivity and studies of argon-only bombardment indicate loss of surface oxygen and the formation of Sn^{2+} and Sn^0 oxidation states at the surface. In the case of aluminum, however, the presence of a significant contact resistance, with consistent adhesion, implies that bonding is via Al–O rather than Al–Sn-based bonds. Given the large dc bias developed during etching (~450 V), ion bombardment (predominantly Ar^+) can be expected to be normal to the tin oxide. Thus the sidewalls are exposed to a lower ion flux, with possibly a lower bombardment energy. Surface conditioning will still occur due to isotropic chlorine neutral species bombardment (Cl and Cl_2), however, studies of chlorine-only plasma etching indicate that the presence of argon-ion bombardment is a major factor in surface modification and etching. Direct measurement of the sidewall surface by XRD and XPS is not possible but it is reasonable to conclude that the enhanced surface reactivity, observed with planar tin oxide, is not replicated to the same extent on the sidewalls. This is supported by observations with copper plating without a reduction process. Plating onto the normal surface indicated better adhesion for the plasma exposed compared to as-deposited tin oxide. However, in neither case was the adhesion or the quality of the plated copper sufficient. XPS and XRD analyses of electrolytically exposed surfaces indicated predominantly the same surface changes as observed due to plasma bombardment. In summary, therefore, it would appear that the inert tin oxide surface precludes significant metal–metal bonding without surface modification and that plasma bombardment alone may not be sufficient, especially for the sidewalls. The use of the electrolytic stage followed by vacuum metal deposition, rather than electroplating, was found to be problematic due to the existence of the resist overhang.

In order to more closely investigate the aluminum to SnO_2 contact resistance, four-point probe I–V studies of the cruciform in the overlapping configuration were employed. Here the voltage across the contact can be monitored at the two passive arms of the cross. In this configuration the interfacial area of the contact at the crossover could be accurately set to $5\times10^4\ \mu m^2$. These devices initially displayed I–V relationships[14] with diodelike characteristic in the first and third quadrants, having a threshold voltage in the range 1.5–3.0 V. On electrically cycling the devices the characteristic quickly changes over approximately six cycles to a stable ohmic characteristic with an ohmic resistance of 700 Ω, a standard deviation of 160 Ω. The associated contact resistivity is very high at $3.5\times10^7\ \Omega\ \mu m^2$. Unlike the previous structures, these crossover devices measure the contact resistance into the top surface of the tin oxide rather than the sidewall and this surface, having been previously covered in resist, is therefore protected against plasma bombardment. Thus the diodelike characteristics and the high contact resistance, three orders of magnitude higher than that measured for the sidewall contact in the abutting configuration, represent the state of the interface between metal and native tin oxide. This suggests both an oxide interface and significant surface modification of the sidewall, the anisotropy of the ion bombardment notwithstanding. Another possibility is that incomplete removal of photoresist, despite rigorous chemical cleaning, may contribute to the high contact resistance.

Further devices were fabricated with an argon sputtered 10–20 nm interlayer of gold, work function 5.1 eV, between the aluminum and the tin oxide. *Ab initio* these samples all exhibited stable, linear, and symmetric I–V relationships with slopes between 0.13 and 0.7 Ω even for first contact voltages in the mV range. The associated contact resistivity range is $6.5-3.5\times10^4\ \Omega\ \mu m^2$. Replication of this cruciform four-point probe topology for 0.4-μm-thick gold alone on top of tin oxide produced a 0.2 Ω linear and symmetric resistance with a contact resistivity $1.0\times10^4\ \Omega\ \mu m^2$. Similarly, evaporated silver, with an almost identical 4.26 eV work function to that of aluminum, gave a contact resistance of 0.04 Ω and contact resistivity of $0.2\times10^4\ \Omega\ \mu m^2$. In neither set of samples produced here was there a ''diodelike'' characteristic or hysteresis; all samples displaying linear ohmic relationships. The contact resistivity of these interlayer devices is of similar magnitude to that of the sidewall aluminum–tin oxide devices measured in the abutting configuration. More detailed investigations are currently in progress into the nature of these contacts but a number of points can be highlighted. Reduced contact resistivity with more noble metals on native tin oxide confirms oxide growth as the mechanism of bond formation with aluminum and indicates photoresist contamination to be negligible. Adhesion of pure Au or Ag contacts are poorer than for Al, while that for the mixed Au–Al shows some improvement and indicates the possibility of optimization between contact re-

sistance and adhesion. It is not clear yet how the aluminum penetrates the Au interlayer to effect improved bonding over the pure Au contact.

IV. CONCLUSIONS

In this article two novel methods of enhancing the conductivity of transparent tin oxide electrodes have been investigated. Both methods apply a low resistivity metal to the sidewalls of the electrode. The application of copper by the electrochemical processes of reduction and plating has been found to be the more successful approach, with a factor of 10 enhancement being achieved. Thus the copper process can find ready application in flat display manufacture especially for large area panels where electroplating represents a solution to the problem of transparent electrode resistance at a similar level of technology to other parts of the panel fabrication process. Aluminum on the other hand, only yields an enhancement of 2. Unlike the case for copper, aluminum was found to have a contact resistance between 0.4 and 1.0 $\times 10^4\ \Omega\ \mu m^2$, which largely accounts for the lower result.

An oxide interlayer between aluminum and the tin oxide is thought to be the main source of the contact resistance and also the reason for the consistently high values of adhesion.

The contact resistance of aluminum to native tin oxide, unexposed to plasma bombardment, is very high, indicating that the plasma bombardment of the tin oxide sidewall is important in forming a lower resistance bond. Surface analysis indicates a change in surface crystal structure and tin oxidation states due to argon–chlorine plasma exposure which would facilitate metal-Sn bonding but it is not clear how the directionality of the ion bombardment reduces the extent of this modification on the sidewall surface. Electroplating of copper onto native tin oxide was not possible without pre-exposure to plasma bombardment or electrolytic reduction, the latter having a more significant effect. Surface analysis of electrolytically reduced tin oxide indicates predominantly the same surface modification as for the plasma but, in this case, the extent of the modification on the sidewall is not expected to vary significantly from that of the top surface of the tin oxide.

Substitution of Au and Ag for aluminum reduced the contact resistance on native tin oxide but also resulted in poorer adhesion. The use of Au–Al contacts indicated the potential for optimization between adhesion and contact resistance. The establishment of a viable vacuum deposited metal-tin oxide lift-off process requires further investigation of suitable contact alloys along with surface modification by either plasma bombardment or electrolytic reduction. In the latter case, the resultant photoresist undercut causes problems with shadowing and must be eliminated.

ACKNOWLEDGMENTS

The authors would like to thank the support provided by Northern Ireland Bioengineering Center and the Northern Ireland Center for Advanced Materials. The Engineering and Physical Sciences Research Council Grant No. Gr/J35412 is also acknowledged as providing financial assistance for this work.

[1]J. A. Farber, S. J. Laverty, A. Eder, and P. Maguire, IEEE Trans. Instrum. Meas. **44**, 918 (1995).
[2]A. Barr and S. J. Laverty, Proc. Inst. Eng. **136**, 173 (1989).
[3]K. Ono, T. Suzuki, H. Sakuta, K. Onisawa, M. Hiroshima, T. Sasaki, M. Tsumura, and N. Konishi, IEICE Trans. Electron. **E79-C**, 1097 (1996).
[4]F. ArefiKhonsari, F. Hellegouarch, and J. Amouroux, J. Vac. Sci. Technol. A **16**, 2240 (1998).
[5]J. Wallinga, W. M. Arnoldbik, A. M. Vredenberg, R. Schropp, and W. F. VanderWeg, J. Phys. Chem. B **102**, 6219 (1998).
[6]A. E. Rakhshani, Y. Makdisi, and H. A. Ramazaniyan, J. Appl. Phys. **83**, 1049 (1998).
[7]L. L. Hope, J. L. Plumb, and D. H. Baird, in Proceedings of Society of Information Display International Conference, Japan, 1983 (unpublished), p. 582.
[8]P. Maguire, J. Molloy, S. J. Laverty, and J. A. McLaughlin, J. Vac. Sci. Technol. B **14**, 3010 (1996).
[9]J. Molloy, P. Maguire, S. J. Laverty, and J. A. McLaughlin, J. Electrochem. Soc. **142**, 4285 (1995).
[10]H. Feng, S. J. Laverty, P. Maguire, J. Molloy, and B. J. Meenan, J. Electrochem. Soc. **143**, 2048 (1996).
[11]R. Shiratsuchi, K. Hongo, G. Nogami, and S. Ishimaru, J. Electrochem. Soc. **139**, 2544 (1992).
[12]N. Inagaki, S. Tasaka, and K. Hibi, J. Polym. Sci., Part A: Polym. Chem. **30**, 1425 (1992).
[13]N. R. Armstrong, A. W. C. Lin, M. Fujihara, and T. Kuwana, Anal. Chem. **48**, 741 (1976).
[14]S. J. Laverty and P. D. Maguire, J. Electrochem. Soc. **147**, 772 (2000).